INVESTIGATION OF THE CLPXP PROTEASE'S CONNECTION TO *BACILLUS*

ANTHRACIS CELL WALL CHARACTERISTICS

by

CHRISTOPHER RYAN EVANS

Bachelor of Science, 2011
Texas Christian University
Fort Worth, Texas

Submitted to the Graduate Faculty of the
College of Science and Engineering
Texas Christian University
in partial fulfillment of the requirements
for the degree of
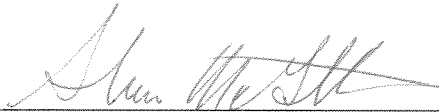

Master of Science

May 2013

INVESTIGATION OF THE CLPXP PROTEASE'S CONNECTION TO *BACILLUS ANTHRACIS* CELL WALL CHARACTERISTICS
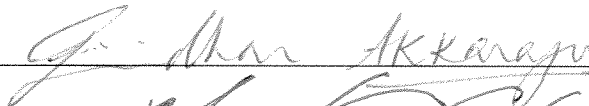
by

Christopher Ryan Evans

Thesis approved:

_____

Major Professor

_____

_____

_____

For The College of Science and Engineering

ACKNOWLEDGEMENTS

TABLE OF CONTENTS

LIST OF FIGURES

Introduction

Bacillus anthracis is a gram-positive, rod-shaped, spore-forming intracellular pathogen and was the first microorganism directly linked to a specific disease, Anthrax, by Robert Koch. This discovery laid the foundation for key concepts of pathogen discovery, called Koch's Postulates (Hart and Beeching, 2002). The term, anthrax, meaning "coal" in Greek, was coined by Hippocrates due to the black lesions formed on the skin of animals with the disease. There are three forms of the disease: subcutaneous, gastrointestinal, and inhalational. Subcutaneous infection is characterized by black lesions on the skin, but only has a 30 percent mortality rate – the lowest of the three forms of the disease (Baillie and Read, 2001). Gastrointestinal anthrax infection is characterized by stomach pain, bloody vomit, and diarrhea. It is acquired by the ingestion of meat tainted by the bacteria or its spores and has a mortality rate of 40 percent. The most serious form of anthrax disease is inhalational infection. The ability of *B. anthracis* to form spores and the ease at which they can be aerosolized, combined with a mortality rate up to 90 percent makes it a major concern for bioterrorism and is classified by the CDC as a Category A pathogen (Hart and Beeching, 2002).

The ability of *B. anthracis* to establish an infection relies on the virulence factors the bacteria possesses. The major virulence factors of *B. anthracis* are its toxins and capsule which are genetically encoded on two extra-chromosomal plasmids, pX01 and pX02 respectively. The bacterial toxins, lethal toxin and edema toxin, enter the cell through endocytosis and impair protein kinase function,

ultimately leading to suppression of the immune response and cell death. The other major virulence factor is the bacterial capsule, which prevents phagocytosis of the bacteria by immune cells, thus preventing the clearance of the infection by the immune system. Despite their significant role in establishing infections by *B. anthracis*, the virulence of the bacteria cannot be fully explained by these two factors. For example, it has been shown that neither of these plasmids contributes to the ability of the bacteria to resist antibiotics or survive inside the macrophage (Dixon et al., 2000). After sequencing the *Bacillus anthracis* genome, a number of genes were found to be homologous to known virulence genes in other pathogens (Read et al., 2003). Based on the results of these studies, it would be worthwhile to investigate potential chromosomal virulence factors in *B. anthracis*.

Previous research has shown that ClpX, a gene coded in the chromosomal region of *B. anthracis*, is necessary for virulence (McGillivray et al., 2009). A genetic knock-out of *clpX* in *B. anthracis (*ΔClpX) showed decreased subcutaneous and inhalational infections in mice (McGillivray et al., 2009). Along with *B. anthracis*, ClpX has been shown to be involved in the virulence of other human pathogens *E.coli, S. aureus,* and *S. pneumonia* (Frees et al., 2007). ClpX is an ATPase that works in conjunction with ClpP to form the ClpXP intracellular protease complex where ClpX forms a hexamer ring on top of a hexamer column of ClpP proteins (Baker and Sauer, 2011). Targeted proteins are unfolded by the ClpX ring and fed into the ClpP column as a peptide string where they are degraded. ClpXP acts as a global regulator within the cell by controlling the levels of various transcription factors and regulatory proteins (Frees et al., 2007). Alone, ClpX acts

as a protein chaperone and has been implicated in bacterial stress responses, protein turn-over, and sporulation (Frees et al., 2007).

In *B. anthracis*, ClpX plays a role in resistance to cell wall-acting antibiotics. The *clpX* mutant, ΔClpX, has an increased susceptibility to cell wall-acting antibiotics, including daptomycin, penicillin, and vancomycin, along with the human antimicrobial peptide, LL-37 (McGillivray et al., 2009). Antimicrobial peptides are proteins in the innate immune system with antimicrobial properties. The antimicrobial peptide LL-37 is a human cathelicidin that is found in phagolysozomes of macrophages. Each of these antimicrobials interact-with or target the cell wall of the bacteria and have different modes of action: daptomycin depolarizes the cell membrane after crossing the cell wall, penicillin and vancomycin act to inhibit peptidoglycan cross-linking, and LL-37 create lethal pores in the bacterial membrane after penetrating the cell wall.

Bacteria respond to and protect themselves against these types of antimicrobial attacks in a variety of ways. A decrease in the autolytic rate of bacteria increases resistance to cell wall-acting antimicrobials. Autolysis is the process of loosening bonds within the cell wall so that bacteria may grow, by the addition of new bonds, or separate, by breaking the bonds at the division site. In *Staphylococcus aureus,* a mutantion in *lrgA* and/or *lrgB*, which are regulated by the *lytSR* two-component regulatory system, has increased autolytic activity, autolysin production, and penicillin susceptibility (Groicher et al., 2000). The authors of the study hypothesized that an increase in autolytic activity resulted in increased breakdown of the peptidoglycan chains and a weaker cell wall. LrgAB is

responsible for controlling the production of autolysins during late stationary phase of growth (Groicher et al., 2000). Another set of genes, *yycF* and *yycG*, have been shown to influence autolysin activity in *S. aureus* and play a role in daptomycin resistance (Martin et al., 1999). In clinical isolates of *S. aureus* that are resistant to daptomycin, YycG was found to have a mutation, potentially decreasing or eliminating its activity (Friedman et al., 2006). Mutations in both *yycF* and *yycG* in *S. aureus* resulted in increased antibiotic susceptibility (Martin et al., 1999). We hypothesize that ClpX works in conjunction with ClpP to affect autolytic activity through regulation of the expression of *lrgAB*, *lytSR*, and/or *yycFG* and is responsible for increasing resistance to cell wall antimicrobials.

An increase in cell wall charge has also been linked to resistance to cationic antimicrobials. Cathelicidins, as well as other antimicrobial peptides, and daptomycin have a net positive charge and an increase in cell wall charge is thought to increase the repulsion of antimicrobials away from the bacterial wall. Increased expression on *mprF*, a gene known to increase cell wall charge in bacteria by incorporating l-lysine into phosphatidylglycerol in the cell envelope, leads to daptomycin and antimicrobial peptide resistance in *S. aureus* (Mishra et al., 2009)*, B. anthracis* (Samant et al., 2009)*,* and *B. subtilis* (Hachmann et al., 2009). An operon, *dltABCD*, expresses proteins that increase cell charge in *Bacillus subtilis*, *Bacillus anthracis,* and *Staphylococcus aureus* (Neuhaus and Baddiley, 2003). These proteins incorporate positively-charged D-alanine residues to cell wall lipotechoic acid, resulting in an increase in cell wall charge (Neuhaus and Baddiley, 2003). We hypothesize that the loss of *clpX* results in a decrease in cell charge due to the

misregulation of *mprF* or *dltABCD*, leading to an increased susceptibility to positively-charged antimicrobials.

An increase in cell wall thickness has been linked to resistance to vancomycin and daptomycin in clinical isolates (Hanaki et al., 1998; Mishra et al., 2011). An increase in cell wall thickness is due to an increase in cell wall biosynthesis pathways (Hanaki et al., 1998). We hypothesize that the loss of *clpX* could result in a misregulation of cell wall biosynthesis or upkeep that could account for the increased cell wall-acting antimicrobial susceptibility.

Methods

Bacterial Strains and Cultures

The parental *B. anthracis* strain used in this study is *B. anthracis* Sterne (pX01[+], pX02[-]). *B. anthracis* ΔClpX is previously described (McGillivray et al., 2009). *B. anthracis* cultures were grown in brain heart infusion (BHI) (Criterion) or Roswell Park Memorial Institute medium (RPMI) (Cellgro) supplemented with 5% Lysogeny broth (LB) at 37° C shaking unless otherwise stated. *S. pyogenes* strains were kindly provided by Victor Nizet (UCSD), and were grown in BHI.

RNA Extraction, cDNA synthesis, and Real Time Quantitative PCR

Bacterial RNA was extracted using RNeasy Mini Kit (Qiagen) per manufacturer's protocol, including the extra RNA elution step, from stationary phase cultures grown in

BHI. The RNA was treated with two rounds of DNase treatment using TURBO DNA-free

Kit. cDNA was made from the extracted RNA using High Efficiency cDNA Synthesis Kit

(Applied Biosystems) per manufacturer's protocol. SYBR Green PCR Mix (Life

Technologies) was used for QPCR (Applied Biosystems 7500 Real-Time PCR System). 40

cycles were used to amplify the target gene using the following protocol.

Stage	Repetitions	Temperature	Time
1	1	50° C	2:00
2	1	95° C	10:00
3	40	95° C	0:15
		60° C	1:00

Primers used are listed in the table below. Relative expression of genes was calculated

using the Livak method (Bio-Rad Laboratories, *Relative Quantification Normalized*

Against a Reference Gene 2012). Briefly,

$\Delta CT_{(Target)} = CT_{(\Delta ClpX, \, Target \, Gene)} - CT_{(WT, \, Target \, Gene)}$ and

$\Delta CT_{(Reference)} = CT_{(\Delta ClpX, \, Reference \, Gene)} - CT_{(WT, \, Reference \, Gene)}$

$\Delta\Delta CT = \Delta CT_{(Target)} - \Delta CT_{(Reference)}$

Normalized Expression = $2^{-\Delta\Delta CT}$

Name of Primer		Sequence
FusA Fwd	-------------	AAG CTG GTG GTG CTG AAG CAC
FusA rev short	-------------	CCA TTT GAG CAG CAC CAG TGA
LrgA Fwd	-------------	CCA ATT CCA ATG CCC TCA TC
LrgA Rev short	-------------	CTG AAA TAC CTG ATG GGA CG
LrgB Fwd	-------------	ATC TCT GAA AGC ATT GGT GG
LrgB Rev short	-------------	GCA TTA GGA GTG GCA GTA GG
LytR Fwd	-------------	ACG ATG GAC ACG CAT GAA AC
LytR Rev short	-------------	ATA TGT AGG GCT TGT GGA CG
LytS Fwd	-------------	CTA TCG RCG GAA TTG GAG TAG G
LytS Rev short	-------------	GAA GAG ATC GCG CAA CTT AGC
YycF Fwd	-------------	AGG TTT ACA AAT GGC CCT GC
YycF Rev short	-------------	TCT TGC TAC TAG CTC ACT CG
YycG Fwd	-------------	TGA TAA GGA TGG TCG TAC AG
YycG Rev short	-------------	GCA ACA ACG TAA ATG GCA CC
mprF Fwd	-------------	TTC GTT CCT CGG TCT TAT CG
MprF Rev short	-------------	CTT GTC CTT CCG CTT GCT TC
DltD Fwd short	-------------	AGA TCA AAC AGG TGC AGC AG
Ba dltD Rev	-------------	CAG GAA CAG AGA TGA AGA GTG G

All experiments were performed with at least 3 independent RNA preparations. Results are presented as the combined average of 3 independent experiments +/- standard error of the mean (SEM).

Triton X-100 Autolysis Assays

Bacterial cultures were grown to an optical density of 0.4 at 600 nm and washed twice in 10mM sodium phosphate buffer (pH 7.0). After washing, bacteria were resuspended in sodium phosphate buffer to a concentration of 2x the original culture volume. They were then incubated at 30°C with an equal volume of 0.1% Triton X-100 detergent in sodium phosphate buffer, making the final concentration of bacteria 1x in 0.05% Triton X-100. Bacterial lysis was measured by optical density at 600 nm every 15 minutes.

Minimal media autolysis assay

Bacterial cultures were grown starting with equal amounts of bacteria from frozen glycerol stocks and OD600 was taken after 48 hours. The minimal media used is a modified Spizizen Minimal Media containing (percentages by weight): 0.2% ammonium sulfate, 1.4% potassium phosphate (dibasic), 0.6% potassium phosphate (monobasic), 0.02% magnesium sulfate, 0.5% Glycerol, 0.02% Casamino acid, and 50µg/mL Tryptophan.

Cell Charge Assays

For the Cytrochrome C assay, bacterial cultures were grown to early log phase, washed in 20 mM MOPS buffer (pH 7.0), then centrifuged and resuspended in 20 mM MOPS buffer to an optical density of 5.0 at 600 nm. They were then incubated with 1 mg/mL cytochrome C for 10 minutes at room temperature in a total volume of 0.5 mL. After incubation, the samples were centrifuged at 16000 rpm for 3 minutes and the optical density of the supernatant was measured at 530 nm to measure residual cytochrome C.

For the poly-L-lysine assay, bacterial cultures were grown to early log phase, washed in 20 mM HEPES buffer (pH 7.5), then centrifuged and resuspended to an optical density of 0.1 at 600 nm. They were then incubated with 10 μg/mL poly-L-lysine for 30 minutes at room temperature in a total volume of 0.5 mL. After incubation, the samples were centrifuged at 16000 rpm for 3 minutes. The fluorescent excitation of the supernatant was measured at 485 nm.

Scanning Electron Microscopy

Bacterial cultures were grown overnight in BHI, washed once in PBS and resuspended and fixed in 1% glutaraldehyde for 1 hour at room temperature. The samples were then dehydrated with a series of 10-minute alcohol incubations at the

following concentrations (in order): 30%, 50%, 70%, 85%, 90%, and 100%. The

incubation with 100% alcohol was performed twice. Next, samples were incubated with

hexamethyldisilazane overnight with the tube lid open to allow excess liquid to

evaporate. The dry pellet was crushed and transferred to a metal pedestal and sputter

coated with 8 nm of gold. Images were taken at 20kV with a JEOL JSM-6100 Scanning

Microscope.

Transmission Electron Microscopy

Bacterial cultures were grown overnight in BHI or RPMI +5% LB and washed in

PBS. Samples were resuspended and fixed in 2.5% glutaraldehyde for 1 hour at room

temperature. Bacterial pellets were then washed in PBS three times. The samples were

incubated in 1% osmium tetroxide for 1.5 hours on ice. Osmium tetroxide was removed

and the samples were dehydrated with a series of 10-minute alcohol washes at the

following concentrations (in order): 30%, 50%, 70%, 85%, 95%, and 100%, repeating the

wash in 100% alcohol three times. Samples were then incubated in 100% propylene

oxide for 15 minutes. Next, the samples were incubated 24 hours at room temperature

in 50% propylene oxide/50% Embed plastic (10g Embed 812, 8g DDSA, 4g NMA, and

0.6g DMP 30). After the 24 hour incubation, the samples were embedded in 100%

plastic and kept at 60° for 72 hours.

90 nm sections were made and placed on copper grids. Sections were stained in

uranyl acetate stain (2g of uranyl acetate in 100 mL of 50% acetone) for 4 minutes.

Sections were washed in 50% acetone, then stained in lead citrate for 4 minutes. Lead

citrate stain was made by dissolving 0.08g of lead citrate in 18 mL of previously-boiled

water and 2 mL of 1.0M NaOH. Sections were washed in 0.05M NaOH, followed by a

wash in previously-boiled water and dried on filter paper. Images were taken at 200kV

using a JEOL 2100 Transmission Electron Microscope.

Results

Rate of Autolysis in ΔClpX

Changes in autolytic rates have been shown
to change bacterial susceptibility and resistance to
antimicrobials that target the cell wall (Groicher
et al., 2000). We hypothesize that an increase in
autolytic rate could be responsible for the
increased antimicrobial susceptibility of ΔClpX.
We first examined the expression of genes
associated with autolysis using quantitative real-
time PCR. We see a significant decrease in *LrgA*

Figure 1. The expression of autolytic genes in ΔClpX in comparison to WT. Three genes, *lrgA, lrgB*, and *yycG*, show significantly different expression in comparison to WT by QPCR. Results shown are the combined average of 3 independent experiments ± SEM. Asterisk denotes p-value < 0.05 by paired t-test.

and *LrgB* expression, which both negatively regulate autolysin activity, and an

increase in *YycG* expression, which has a positive r egulatory role in autolysin

activity, in ΔClpX in comparison to WT (Figure 1). We see no significant change in

yycF, a gene within the same regulon as *yycG*, or in the two-component regulatory
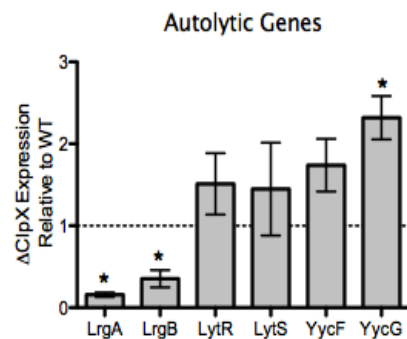
system, *lytR* and *lytS*. These results show that genes associated with autolysis are misregulated after the loss of *clpX*. The genes misregulated, *lrgA, lrgB,* and *yycG*, all have changes in expression that indicate an increase in autolytic rate and support our hypothesis.
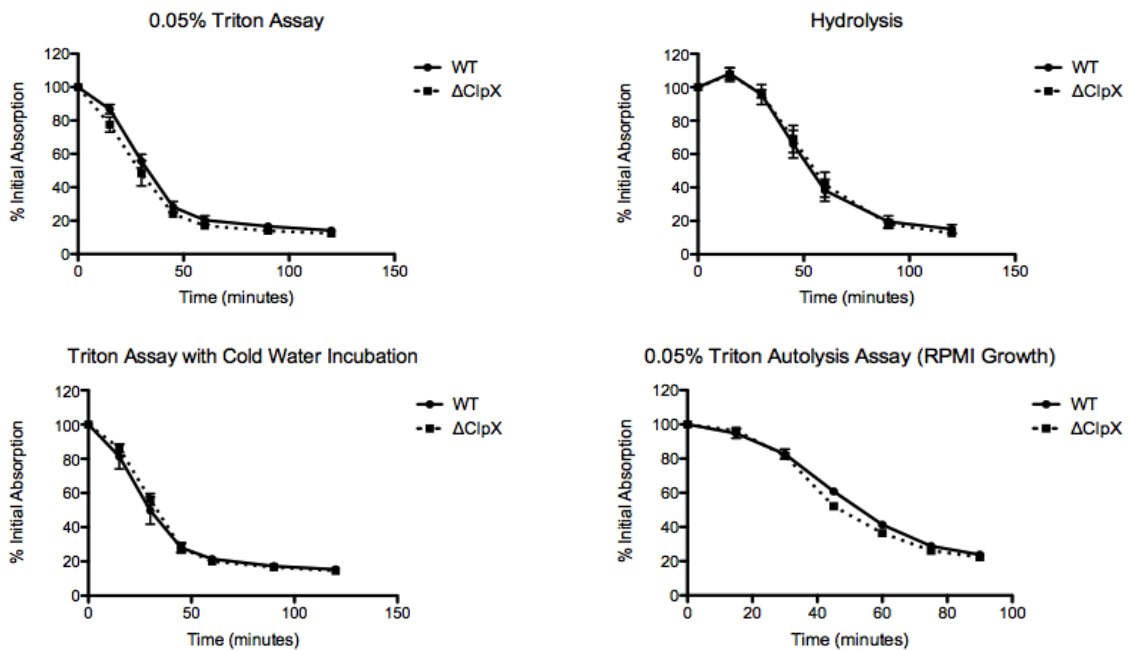

Figure2. No difference in autolysis rate between WT and ΔClpX after BHI growth. Log phase WT and ΔClpX *B. anthracis* were incubated in (A) 0.05% Triton X-100, (B) ice cold water, or (C) cold water then 0.05% Triton X-100. Bacteria grown in RPMI +5% LB were incubated in (D) 0.05% Triton X-100. OD600 was measured every 15 minutes and relative survival was determined based on the initial measurement. Figures are combined averages of 3 independent experiments ± SEM.

To determine the actual autolytic rates in the ΔClpX mutant, we conducted a series of Triton X-100 autolysis assays. Triton X-100 is a detergent used to induce autolysis by causing the release of lipoteichoic acid, a known inhibitor of autolysin function, from the cell membrane, effectively increasing the autolytic rate until lysis occurs (Raychaudhuri and Chatterjee, 1985). The comparative lytic rates after incubation with Triton X-100 can then be used as a proxy for base autolytic rates

between different bacteria. After

exposure to 0.05% Triton X-100, both

WT and ΔClpX had similar lytic rates

(Figure 2, A). In order to determine if

hydrolysis played any role in autolytic

rates we measured cell death during

incubation in cold water over 120

minutes (Figure 2, B) and looked at

Triton X-100 induced autolytic lysis

Minimal Media Autolysis

Figure 3. ΔClpX has an increased lytic rate after long term growth in minimal media. Over 48 hour growth in Spizizen Minimal Media, ΔClpX has decreased growth in comparison to WT. Results shown are the combined averages of 3 independent experiments ± SEM. Asterisk denotes a p-value < 0.05 by unpaired T-test.

after a short incubation in cold water (Figure 2, C). Neither of these experiments

showed any difference in autolysis rate between WT and ΔClpX.

Since autolytic rates may be affected by the environment that the bacteria

are grown in, we grew WT and ΔClpX in the cell culture media, RPMI, supplemented

with 5% LB. This media provides a more stressful environment, due to its lack of

nutrients, for the bacteria and can provide us with information about how the

bacteria may respond to an environment more similar to its host than BHI. After

growth in RPMI+5% LB, we found no difference between WT and ΔClpX Triton X-

100 induced autolytic killing (Figure 2, D). In *B. subtilis*, a *yoeB* mutant, a gene

involved in the stress response of bacteria to cell-wall antibiotic attack, was found to

have increased autolytic activity after antibiotic attack or nutrient stress (Salzberg

and Helmann, 2007). Therefore, we also measured long-term stationary-phase

survival after growth in minimal media (Figure 3) to see how ΔClpX can respond to

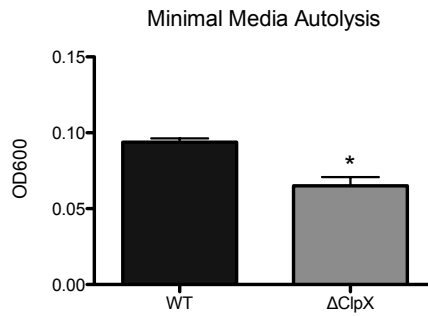low-nutrient-induced stress. After 48 hours, ΔClpX has significantly higher autolytic

death than WT. Based on these results, it is clear that Triton X-100 induced

autolysis is unchanged during normal growth in BHI or growth in RPMI+5% LB.

Further studies need to be done to d etermine whether the autolysis during

nutrient-starvation could play a role in the increased susceptibility of ΔClpX.

Determination of Cell Charge Changes in ΔClpX

We hypothesize that a decrease in the cell charge of the ΔClpX *B.* anthracis mutant could be responsible for its increased susceptibility to cell-wall acting antimicrobials. To begin the analysis of cell charge changes in ΔClpX, we examined 2 genes known to affect cell charge using quantitiative real-
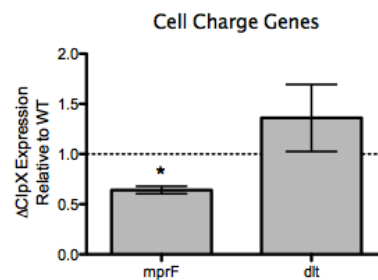

Figure 4. Expression of genes shown to affect cell wall charge in ΔClpX in comparison to WT. In ΔClpX, *mprF* has decreased expression compared to WT expression (shown as dotted line), while *dlt* has no significant change as shown via QPCR. Results shown are a combined average of 3 independent experiments ± SEM. Asterisk denotes a p-value < 0.05 by paired T-test.

time PCR (Figure 4). The gene, *mprF*, known to increase membrane charge by

incorporating l-lysine into phosphatidylglycol (Ernst et al., 2009) , showed

significantly decreased expression in ΔClpX. The *dlt* gene, known to affect cell chage

by substituting positively charged amino acids into the cell wall, showed no

significant changes in expression.

In order to directly measure cell charge, we used cytochrome C, a positively

charged red molecule. After incubating the bacteria with cytochrome C, the

molecule will bind to the cell wall depending on the net charge of the cell. More

cytochrome C will bind to a cell that is more negatively charged and will be repeled

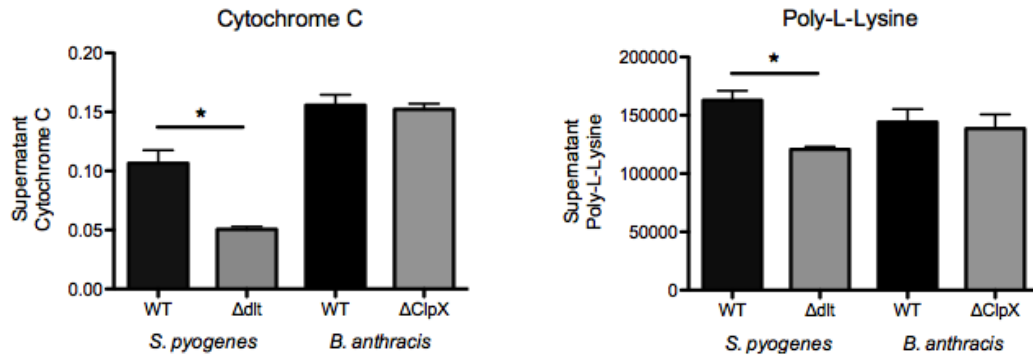by a cell that is more positively charged. The "redness" of the supernatant, which

Figure 5. No difference in cell wall charge between WT and ΔClpX *B. anthracis*. Stationary phase *S. pyogenes* and log phase *B. anthracis* were grown in BHI and equal numbers of bacteria were incubated with (left) 1 mg/mL Cytochrome C or (right) 10 ug/mL Poly-L-lysine. Results shown as OD530 and Fluorescent units, respectively, and are the combined averages of 3 independent experiments ± SEM. Asterisk denotes a p-value < 0.05 by paired T-test.

correlates with cytochrome C levels, can be measured by reading the optical density

at 530nm. Therefore, we can determine cytochrome C levels in the supernatant

versus bound to the cells. As a positive control for the assay, we used WT and Δdlt *S. pyogenes*, strains previously shown to have changes in cell wall charge and obtained

the expected results (Figure 5, left). However, cytochrome C bound equally to WT

and ΔClpX, indicating that there is no net difference in cell charge seen in this assay

(Figure 5, left).

As a way to ensure our cytochrome C results were correct, we used a poly-L-

lysine assay to measure cell charge. Poly-L-Lysine is a positively charged

fluorescent molecule that, like cytochrome C, will bind to a cell based on how

negatively charged it is. After incubating the bacteria with poly-L-lysine, we

measured the fluorescence in the supernatant to determine how much remained

bound to the cells (Figure 5, right) and used the relative fluorescence to determine

the relative cell charge of WT and ΔClpX *B. anthracis*, although our positive control

using WT and Δdlt *S. pyogenes* worked as expected. After incubation, we see no

difference in poly-L-lysine in the

supernatant between WT and

ΔClpX. To examine whether the

growth environment has an

effect on the cell charge of the

ΔClpX mutant, we repeated the

cytochrome C assay after growth

in RPMI+5% LB. There was no

difference in supernatant

cytochrome C between WT and

Figure 6. Growth in RPMI does not induce cell wall charge difference in ΔClpX. Stationary phase bacterial cultures grown in RPMI +5% LB were incubated in 1 mg/mL Cytochrome C and OD530 was taken of the supernatant after centrifugation. Results shown are the combined averages of 3 independent experiments ± SEM. Asterisk denotes a p-value < 0.05 by paired T-test.

ΔClpX after growth in RPMI+5% LB (Figure 6). Based on the results of our

cytochrome C and poly-L-lysine test, we determined that cell charge does not play a
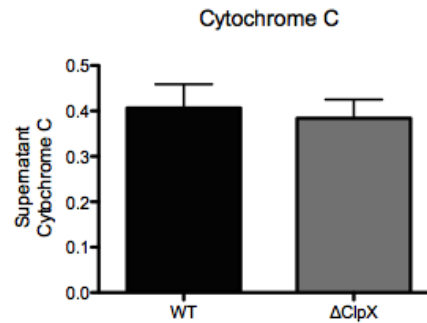
role in the antibiotic susceptibility of ΔClpX.

Examination of ΔClpX Cellular Morphology Using Electron Microscopy

We next examined whether there were physical differences in cellular

morphology between WT and ΔClpX using scanning electron microscopy. Based on

our scanning electron micrographs, we found no obvious differences in size, length,

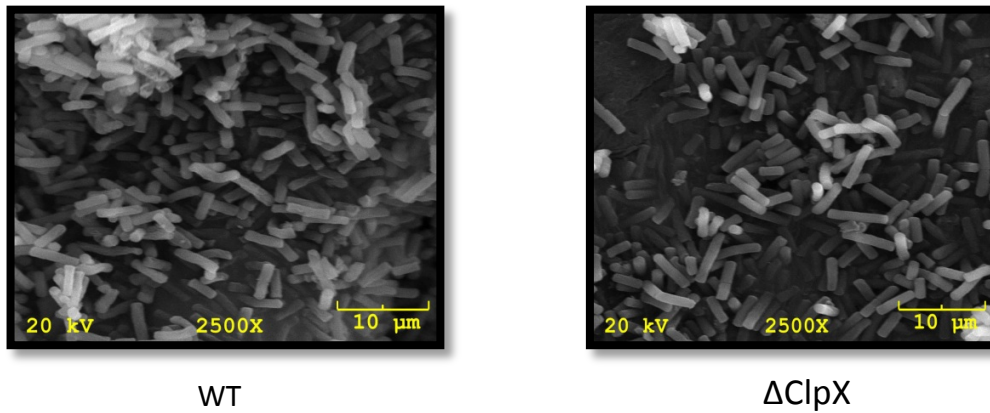or basic shape between stationary phase WT and ΔClpX (Figure 7).

WT   ΔClpX

Figure 7. Scanning electron microscopy shows no difference in basic cell shape between WT and ΔClpX *B. anthraics*. Scanning electron micrographs of stationary phase (A) WT and (B) ΔClpX grown in BHI. Bacterial samples were visualized at 20kV with 2500x magnification.

We next measured cell wall thickness using transmission electron microscopy. Cell wall thickness has been shown to influence *S. aureus* resistance and susceptibility to cell wall-acting antimicrobials, such as vancomycin and daptomycin. We viewed bacterial cell walls after growth in BHI, and after growth in RPMI+5% LB to determine whether environmental affects play a role in cell wall

Wild Type   ΔClpX
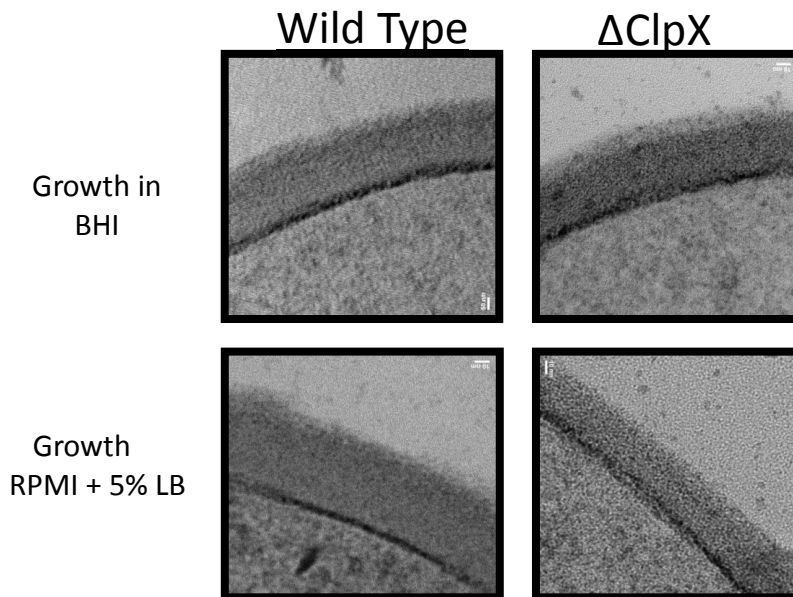
Growth in BHI

Growth RPMI + 5% LB

Figure 8. Transmission electron microscopy indicates a difference in cell wall thickness between WT and ClpX after growth in RPMI. Stationary phase (left column) WT and (right column) ΔClpX *B. anthracis* were grown in (top row) BHI or (bottom row) RPMI +5% LB. Sections were visualized at 200kV at 120,000x magnification.

17

thickness (Figure 8). Upon initial examination, ΔClpX grown in RPMI+5% LB appeared substantially thinner than WT grown in RPMI+5% LB or either strain grown in BHI.

To quantitate cell wall thickness, we measured multiple cell wall cross-sections from both bacterial strains. Initial images were taken at 2000x magnification (Figure 9, A), then circular cross sections where t he cell membrane and end of the cell wall were clear were identified. In order to measure the cell walls more precisely, zoomed-in images were taken at 6000x of the bacteria that were within the clarity parameters (Figure 9, B). To take the measurement, a linear profile was taken across the cell membrane and cell wall. The resulting histogram of
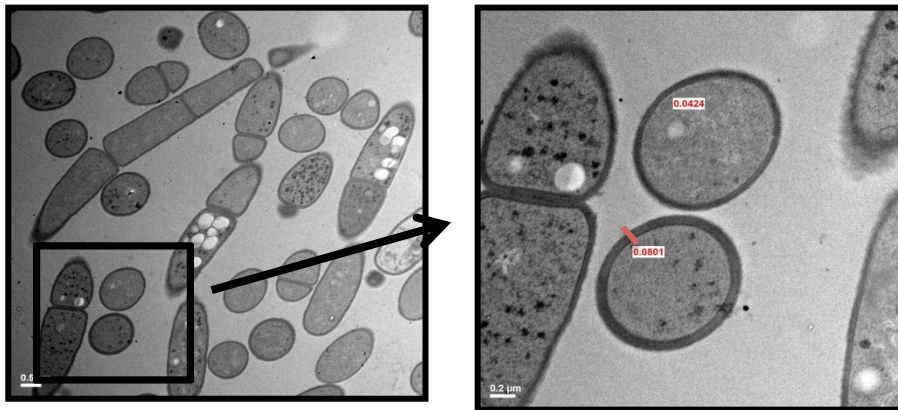
Figure 9. Method for measuring cell wall thickness. Large scale screens were taken at (A) 2000x magnification, then images were taken of (B) each circular cross sectioned bacteria at 6000x magnification. Cell wall thickness measurements were collected by taking a linear profile of each cell wall, represented by (C) a histogram of electron densities along that line. Measurements were taken from the beginning of the membrane to the end of the cell wall, as shown by the dotted lines.
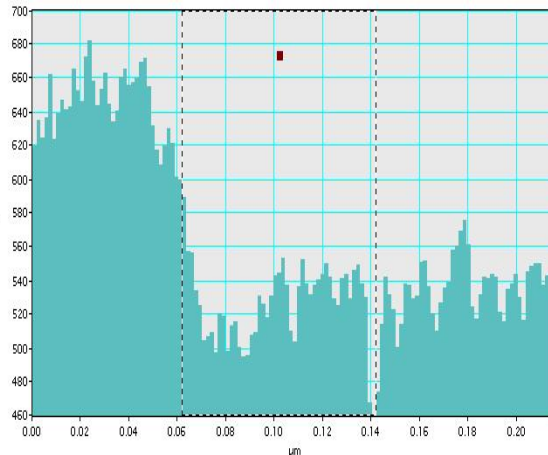
the profile precisely shows the cell membrane, indicated by very low electron beam

counts due to its dark stain, and the end of the cell wall, indicated by a sharp

increase in electron beam counts (Figure 9, C). Clicking and dragging from the

beginning of the membrane to the end of the wall on the histogram produced a

measurement of thicknes s. Our measurements show a significant difference in cell

wall thickness between WT and ΔClpX after growth in BHI and RPMI+5% LB,

although the difference in BHI is smaller. After growth in RPMI+5% LB, we

measured 79 WT and 93 ΔClpX bacteria and found that the cell wall of WT is 59.9 ±

11.4 nm and of ΔClpX is 52.0 ± 8.6 nm, a difference of 13.3%. This difference is much

greater than the difference seen after growth in BHI, where the cell wall of ΔClpX is

only 5% thinner (Figure 10). Therefore, we conclude that the cell wall of ΔClpX is

thinner than WT. This decrease in cell wall thickness may play a role in its

increased susceptibility of ΔClpX to cell wall-acting antimicrobials.
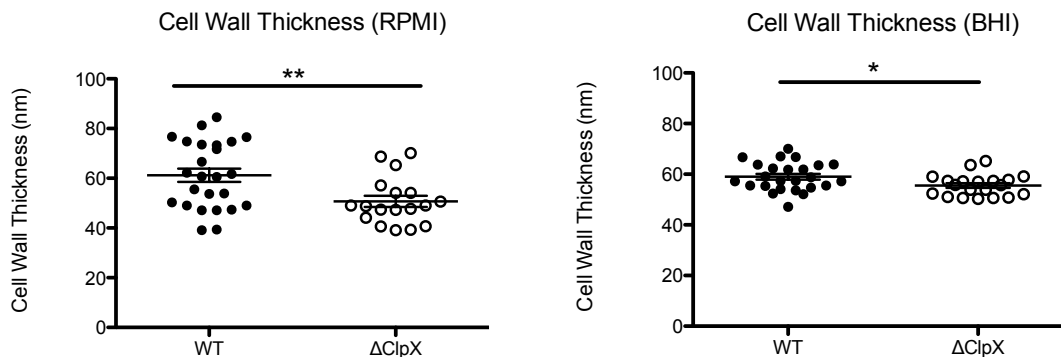
Figure 10. Cell wall thickness is decreased in ΔClpX. Cell wall thickness measurements taken from transmission electron microscopy images after bacteria were grown overnight in RPMI+5% LB (left) or BHI (right). Asterisk denotes a p-value < 0.05 and double asterisk denotes a p-value < 0.01 by unpaired T-test.

Besides the difference in average cell wall thickness, the range and variation

in cell wall thickness was different between WT and ΔClpX (Figure 10, left, Figure

11, A). When plotted in a histogram, cell wall thickness measurements from WT

bacteria grown in RPMI+5% LB show a bimodal curve with a peak at 55 nm and a

peak at 75 nm (Figure 11, B). The cell wall thickness measurements of ΔClpX

bacteria show a single peak at 50 nm (Figure 11, C).

Figure 11. Variation in cell wall thickness after growth in RPMI. (A) Combined measurements of cell wall thicknesses of WT and ΔClpX grown overnight in RPMI+5% LB from 3 independent experiments. T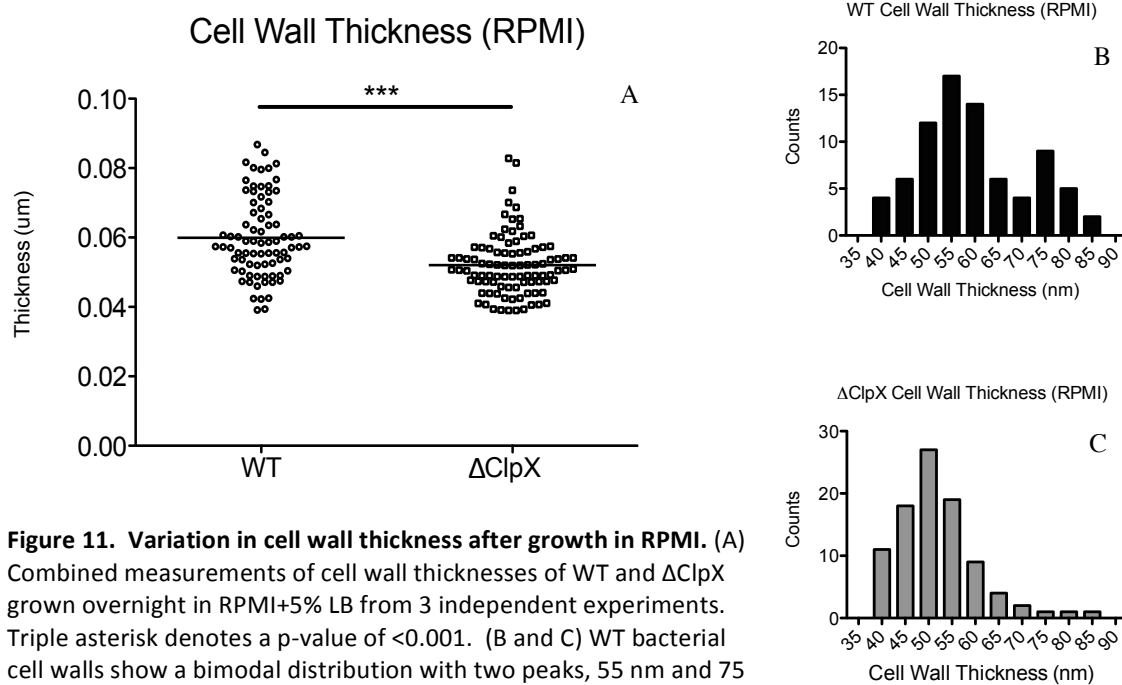riple asterisk denotes a p-value of <0.001. (B and C) WT bacterial cell walls show a bimodal distribution with two peaks, 55 nm and 75 nm (B). ΔClpX bacterial cell wall thickness shows a bell curve distribution skewed to the right with a single peak at 50 nm (C). Data is combined from three independent experiments.

We looked at the physical cell wall response of the two strains of bacteria to

antimicrobial attack by examining them after ove rnight growth in RPMI+5% LB

with 0.8 µM LL-37. In WT, we observed prominent cell wall thickening at the polar

regions (Figure 12, A), but not in ΔClpX. LL-37 preferentially binds to division sites

(Sochacki et al., 2011), so thickening around these sites could provide resistance

and result in thicker polar regions after separation. LL-37-induced-killing resulted

in the cell membranes pulling away from the polar regions before the midcell

regions in both WT and ΔClpX (Figure 12, B-D). This indicates that the polar

membrane may be the first area affected by LL-37 attack. Cell wall breaking, a sign associated with cell death, consistently happened near the polar region, but never in an area of increased cell wall thickness (Figure 12, B,C, indicated by arrows). This

Wild Type   ΔClpX
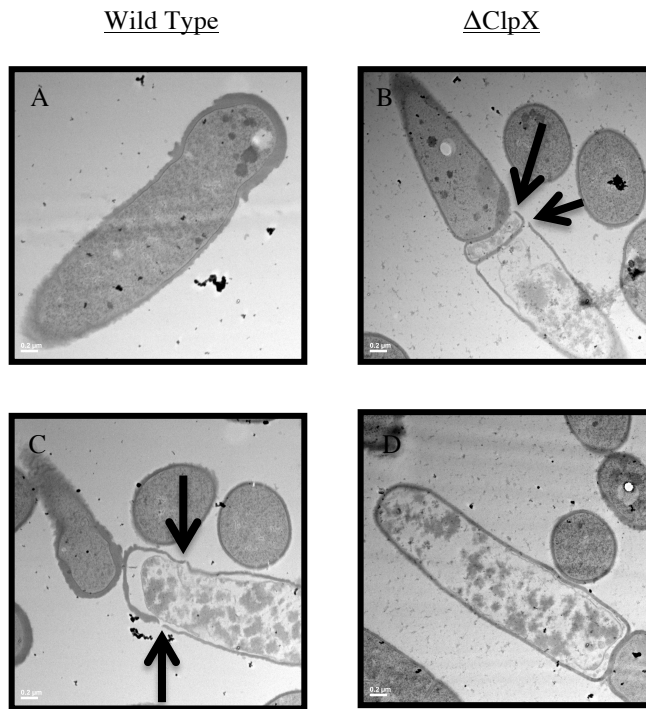
Figure 12. WT has thickened poles after exposure to LL-37. WT and ΔClpX were grown overnight in RPMI+5% LB with 0.8 μg/mL LL-37. Cell wall breaking and cell membrane retraction are indicated by black arrows.

indicates that the thickened cell wall provides physical strength to the bacteria and may help resist death by lysis. We conclude that WT seems to respond to LL-37 attack and ClpX must play a role in that response.

Unexpectedly, we also observed abnormal cell division defects in ΔClpX that were not seen in WT. Interestingly, this was only observed when ΔClpX is grown in RPMI+5% LB. No division defects were seen in BHI. During normal division, a cell has a single division plane in the center of the cell, resulting in two equally sized bacteria (Figure 13, left). During the division of ΔClpX bacteria we see multiple division planes located at the poles, resulting in the formation of minicells (Figure 13, A and B). The reason behind the minicell formation in ΔClpX after growth in

Wild Type   ΔClpX
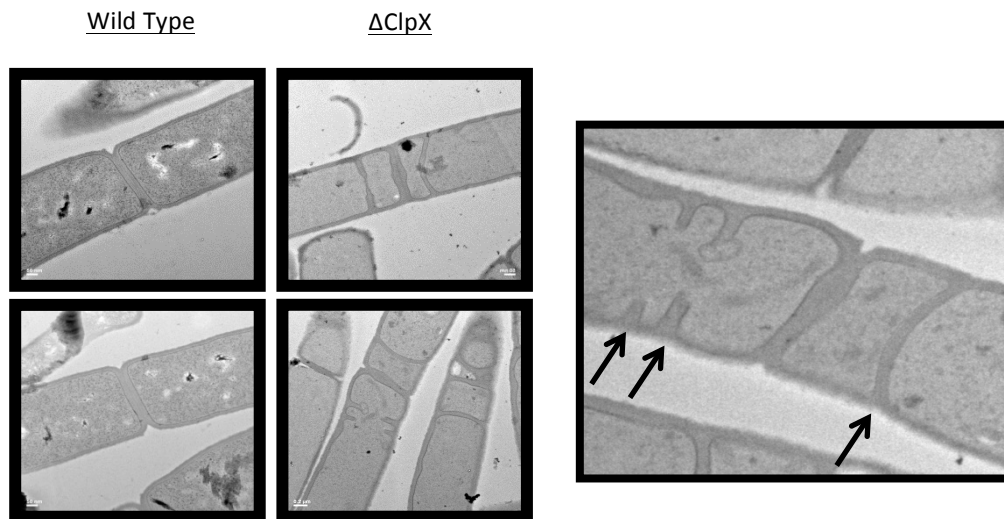
Figure 13. Growth in RPMI causes abnormal cell division in ΔClpX. TEM images show an increased number of divisions per division site in ΔClpX (A, right) *B. anthracis* after growth in RPMI+5% LB. In WT (A, left) division occurs normally. (B) Increased magnification of ΔClpX grown in RPMI+5% LB. Arrows indicate abnormal division sites.

RPMI+5% LB, but not BHI, is unclear; however, RPMI is a more stressful environment than BHI, and contains a number of ingredients not found in BHI. Sodium bicarbonate is found in RPMI, but not BHI, and can change the antimicrobial susceptibility of bacteria (Dorschner et al., 2006) so we tested its ability to induce minicell formation. We grew WT and ΔClpX in BHI with 10 μg/mL sodium bicarbonate and in RPMI+5% LB and examined cell division using phase contrast microscopy (data not shown). We were able to confirm minicell formation in ΔClpX after growth in RPMI+5% LB, but saw no minicell formation in WT or ΔClpX in BHI with sodium bicarbonate, indicating that sodium bicarbonate is not the causative factor for minicell formation.

Discussion

Previous studies have shown that autolytic rate, cell charge, and cell wall thickness can affect bacterial susceptibility to cell wall-acting antimicrobials. We have evaluated each of these characteristics in ΔClpX *B. anthracis*, which was previously shown to have an increased susceptibility to cell wall-acting antimicrobials (McGillivray et al., 2007). We have found that there is no difference in autolytic rate or cell charge between WT and ΔClpX, indicating that changes in these characteristics are likely not the cause of the increased susceptibility.

Based on our transmission electron micrographs, we have concluded that the cell wall of ΔClpX is significantly thinner than WT. This is seen after growth in BHI and RPMI, although the difference in RPMI is much greater. An increased cell wall thickness is thought to play a role in antimicrobial resistance by preventing the antimicrobials from physically reaching their target (Yang et al., 2011). Increased thickness in cell walls has been seen in strains of daptomycin-resistant and vancomycin-resistant *S. aureus* (Hanaki et al., 1998). Because we see a bigger difference in cell wall thickness after growth in RPMI than in BHI, the decrease in ΔClpX cell wall thickness may be due to the inability to properly respond to the stress caused by a specific environment. It has been shown that the environment in which the bacteria are grown affects bacterial susceptibility to LL-37; specifically the presence of bicarbonate, a key ionic factor in mammalian tissues (Dorschner et al., 2006). This study showed changes in *S. aureus* and *E. coli*, including thinner cell walls, after growth in media supplemented

with bicarbonate that increased their susceptibility to LL-37. RPMI does contain

bicarbonate although BHI does not and this could contribute to the difference seen in

ΔClpX grown in BHI vs. RPMI. However, it may also be a combination of stressors as we

supplement BHI with bicarbonate but did not see any noticeable difference in the ClpX

Δmutant.

In WT *B. anthracis* we see a substantially increased cell wall thickness at the

bacterial poles after growth in RPMI with the antimicrobial peptide LL-37 in comparison

to ΔClpX. In *E. coli,* LL-37 preferentially binds to cell poles before penetrating the

bacteria (Sochacki et al., 2011). The increased polar cell walls in WT after incubation

with LL-37 and RPMI could make it more difficult for LL-37 to preferentially puncture the

polar cell membrane, resulting in increased LL-37 resistance. This hypothesis is

supported by our images showing the cell wall bursting immediately interior to the

thickened cell wall poles in WT bacteria. Therefore, we conclude that ClpX is likely

necessary for cell wall biosynthesis under stressful conditions. The exact targets of ClpX

are unknown, but the loss of *clpX* could prevent the initiation of increased cell wall

biosynthesis, or by hampering the increased cell wall biosynthesis directly. This may

result in a relatively weaker cell wall than WT, leading to increased susceptibility to

antimicrobial attack.

Interestingly, we only see the pronounced cell division defect in ΔClpX after

growth in RPMI, but not BHI media. ClpX has been shown to degrade FtsZ, a protein

that polymerizes to form a ring at the midcell immediately prior to bacterial division in

E. coli (Camberg et al., 2011). ClpX also regulates FtsZ assembly in *B. subtilis* in a ClpP-

independent manner (Weart et al., 2005). The loss of *clpX* would prevent the

degradation of FtsZ rings after normal cell division, leading to more division sites, which

is consistent with the minicell formation we see in ΔClpX. In *E. coli*, overproduction of

FtsZ within a certain range has been linked to minicell formation (Ward and

Lutkenhaus, 1985). However, the formation of extra division sites at the poles indicates

that the MinCDE system is another potential target of ClpX. This system is responsible

for the prevention of minicell formation under normal conditions (Goehring and

Beckwith, 2005). In this system, MinC inhibits FtsZ polymerization, therefore preventing

cell division. To prevent division at the poles, MinC oscillates within the cell, spending a

majority of the time in the pole regions, thus preventing FtsZ ring formation at the cell

poles and ensuring division at the midcell (Goehring and Beckwith, 2005). Loss of the

MinC in *Bacillus subtilis* results in mini-cell formation due to the increased stabilization

of FtsZ (van Baarle and Bramkamp, 2010). Loss of ClpX could affect the regulation of

the Min system, potentially by degrading a MinC inhibitor. In *E. coli*, the loss of ClpX in

addition to the loss of MinC has similar FtsZ turnover rates, but slower division rates, as

compared to a mutant in MinC alone, suggesting that ClpX has another target within the

cell division machinery (Camberg et al., 2011). To test this, we plan on creating a MinC

knockout strain of *B. anthracis* and determining the phenotypic similarities and

differences it has in comparison to ΔClpX. If our hypothesis is correct, we should see a

similar increased susceptibility to antimicrobials and cell division defects after stressful

growth.

The increased cell wall biosynthesis associated with increased division may provide an increase in number of cell wall-acting antimicrobial targets, especially for antimicrobials known to target poles like LL-37. Since LL-37 preferentially binds to division sites (Sochacki et al., 2011), the increase in division site number in ΔClpX may contribute to its increased susceptibility to LL-37. A metabolic mutant in *E. coli* showed abnormal septum formation when starved of D-alanine, an amino acid incorporated into bacterial cell walls, and had an increased susceptibility to penicillin and lysozyme, suggesting that physiological changes in division and cell wall biosynthesis can affect cell wall-acting antimicrobial susceptibility (Lazdunski and Shaprio, 1972).

We propose a model of ClpX acting within multiple pathways that potentially play a role in antimicrobial susceptibility. In response to environmental stress, including exposure to antimicrobial peptides and growth in rigorous media, the cell may signal to initiate cell wall biosynthesis. The increased biosynthesis results in an increased cell wall thickness, possibly thickening specifically at the cell pole. This thickening prevents antimicrobials from reaching their cell membrane targets. Loss of ClpX may somehow disrupt this process, leading to increased susceptibility to cell wall-targeting antimicrobials. ClpX could also play a role in preventing cell division during stressful or stationary phase growth conditions. The loss of *clpX* leads to increased division septum formation, leading to the formation of minicells either by lacking FtsZ degradation or decreasing MinC levels. This increase in division sites may provide more potential targets for antimicrobials, leading to increased susceptibility to cell wall-acting antimicrobials.

ClpX is a potentially interesting therapeutic target both because of its necessity for virulence but also for antibiotic resistance; however it is unclear why ClpX is so important for both these functions. This work has illuminated one particular role for ClpX in cell wall synthesis and/or cell division. Future research will hopefully continue to decipher the extensive functions ClpX has in the cell and potentially identify additional targets.

References

Baillie, L., and Read, T.D. (2001). Bacillus anthracis, a bug with attitude!. Curr Opin Microbiol *4*, 78-81.

Baker, T.A., and Sauer, R.T. (2011). ClpXP, an ATP-powered unfolding and protein-degradation machine. Biochim Biophys Acta

Camberg, J.L., Hoskins, J.R., and Wickner, S. (2011). The interplay of ClpXP with the cell division machinery in Escherichia coli. J Bacteriol *193*, 1911-18.

Dixon, T.C., Fadl, A.A., Koehler, T.M., Swanson, J.A., and Hanna, P.C. (2000). Early Bacillus anthracis-macrophage interactions: intracellular survival survival and escape. Cell Microbiol *2*, 453-463.

Dorschner, R.A., Lopez-Garcia, B., Peschel, A., Kraus, D., Morikawa, K., Nizet, V., and Gallo, R.L. (2006). The mammalian ionic environment dictates microbial susceptibility to antimicrobial defense peptides. FASEB J *20*, 35-42.

Ernst, C.M., Staubitz, P., Mishra, N.N., Yang, S.J., Hornig, G., Kalbacher, H., Bayer, A.S., Kraus, D., and Peschel, A. (2009). The bacterial defensin resistance protein MprF consists of separable domains for lipid lysinylation and antimicrobial peptide repulsion. PLoS Pathog *5*, e1000660.

Frees, D., Savijoki, K., Varmanen, P., and Ingmer, H. (2007). Clp ATPases and ClpP proteolytic complexes regulate vital biological processes in low GC, Gram-positive bacteria. Mol Microbiol *63*, 1285-295.

Friedman, L., Alder, J.D., and Silverman, J.A. (2006). Genetic changes that correlate with reduced susceptibility to daptomycin in Staphylococcus aureus. Antimicrob Agents Chemother *50*, 2137-145.

Goehring, N.W., and Beckwith, J. (2005). Diverse paths to midcell: assembly of the bacterial cell division machinery. Curr Biol *15*, R514-526.

Groicher, .H., Firek, .A., Fujimoto, .F., and Bayles, .W. (2000). The Staphylococcus aureus lrgAB Operon Modulates Murein Hydrolase Activity and Penicillin Tolerance. J Bacteriol *182*, 1794-1801.

Hachmann, A.B., Angert, E.R., and Helmann, J.D. (2009). Genetic analysis of factors affecting susceptibility of Bacillus subtilis to daptomycin. Antimicrob Agents Chemother *53*, 1598-1609.

Hanaki, H., Kuwahara-Arai, K., Boyle-Vavra, S., Daum, R.S., Labischinski, H., and Hiramatsu, K. (1998). Activated cell-wall synthesis is associated with vancomycin

resistance in methicillin-resistant Staphylococcus aureus clinical strains Mu3 and Mu50. Journal of Antimicrobial Chemotherapy *42*, 199-209.

Hanaki, H., Kuwahara-Arai, K., Boyle-Vavra, S., Daum, R.S., Labischinski, H., and Hiramatsu, K. (1998). Activated cell-wall synthesis is associated with vancomycin resistance in methicillin-resistant Staphylococcus aureus clinical strains Mu3 and Mu50. Journal of Antimicrobial Chemotherapy *42*, 199-209.

Hart, C.A., and Beeching, N.J. (2002). A spotlight on anthrax. Clin Dermatol *20*, 365-375.

Hart, C.A., and Beeching, N.J. (2002). A spotlight on anthrax. Clin Dermatol *20*, 365-375.

Lazdunski, C., and Shaprio, B.M. (1972). Relationship between permeability, cell division, and murein metabolism in a mutant of Escherichia coli. J Bacteriol *111*, 499-509.

Martin, P.K., Li, T., Sun, D., Biek, D.P., and Schmid, M.B. (1999). Role in cell permeability of an essential two-component system in Staphylococcus aureus. J Bacteriol *181*, 3666-673.

Martin, P.K., Li, T., Sun, D., Biek, D.P., and Schmid, M.B. (1999). Role in cell permeability of an essential two-component system in Staphylococcus aureus. J Bacteriol *181*, 3666-673.

McGillivray, S.M., Ebrahimi, C.M., Fisher, N., Sabet, M., Zhang, D.X., Chen, Y., Haste, N.M., Aroian, R.V., Gallo, R.L., et al. (2009). ClpX contributes to innate defense peptide resistance and virulence phenotypes of Bacillus anthracis. J Innate Immun *1*, 494-506.

McGillivray, S.M., Ebrahimi, C.M., Fisher, N., Sabet, M., Zhang, D.X., Chen, Y., Haste, N.M., Aroian, R.V., Gallo, R.L., et al. (2009). ClpX contributes to innate defense peptide resistance and virulence phenotypes of Bacillus anthracis. J Innate Immun *1*, 494-506.

McGillivray, S.M., Thackray, V.G., Coss, D., and Mellon, P.L. (2007). Activin and glucocorticoids synergistically activate follicle-stimulating hormone beta-subunit gene expression in the immortalized LbetaT2 gonadotrope cell line. Endocrinology *148*, 762-773.

Mishra, N.N., McKinnell, J., Yeaman, M.R., Rubio, A., Nast, C.C., Chen, L., Kreiswirth, B.N., and Bayer, A.S. (2011). In vitro cross-resistance to daptomycin and host defense cationic antimicrobial peptides in clinical methicillin-resistant Staphylococcus aureus isolates. Antimicrob Agents Chemother *55*, 4012-18.

Mishra, N.N., Yang, S.J., Sawa, A., Rubio, A., Nast, C.C., Yeaman, M.R., and Bayer, A.S. (2009). Analysis of cell membrane characteristics of in vitro-selected daptomycin-resistant strains of methicillin-resistant Staphylococcus aureus. Antimicrob Agents Chemother *53*, 2312-18.

Neuhaus, F.C., and Baddiley, J. (2003). A continuum of anionic charge: structures and functions of D-alanyl-teichoic acids in gram-positive bacteria. Microbiol Mol Biol Rev *67*, 686-723.

Neuhaus, F.C., and Baddiley, J. (2003). A continuum of anionic charge: structures and functions of D-alanyl-teichoic acids in gram-positive bacteria. Microbiol Mol Biol Rev *67*, 686-723.

Raychaudhuri, D., and Chatterjee, A.N. (1985). Use of resistant mutants to study the interaction of triton X-100 with Staphylococcus aureus. J Bacteriol *164*, 1337-349.

Read, T.D., Peterson, S.N., Tourasse, N., Baillie, L.W., Paulsen, I.T., Nelson, K.E., Tettelin, H., Fouts, D.E., Eisen, J.A., et al. (2003). The genome sequence of Bacillus anthracis Ames and comparison to closely related bacteria. Nature *423*, 81-86.

Salzberg, L.I., and Helmann, J.D. (2007). An antibiotic-inducible cell wall-associated protein that protects Bacillus subtilis from autolysis. J Bacteriol *189*, 4671-680.

Samant, S., Hsu, F.F., Neyfakh, A.A., and Lee, H. (2009). The Bacillus anthracis protein MprF is required for synthesis of lysylphosphatidylglycerols and for resistance to cationic antimicrobial peptides. J Bacteriol *191*, 1311-19.

Sochacki, K.A., Barns, K.J., Bucki, R., and Weisshaar, J.C. (2011). Real-time attack on single Escherichia coli cells by the human antimicrobial peptide LL-37. Proc Natl Acad Sci U S A *108*, E77-E81.

van Baarle, S., and Bramkamp, M. (2010). The MinCDJ system in Bacillus subtilis prevents minicell formation by promoting divisome disassembly. PLoS One *5*, e9850.

Ward, J.E., and Lutkenhaus, J. (1985). Overproduction of FtsZ induces minicell formation in E. coli. Cell *42*, 941-49.

Weart, R.B., Nakano, S., Lane, B.E., Zuber, P., and Levin, P.A. (2005). The ClpX chaperone modulates assembly of the tubulin-like protein FtsZ. Mol Microbiol *57*, 238-249.

Yang, H., Sikavi, C., Tran, K., McGillivray, S.M., Nizet, V., Yung, M., Chang, A., and Miller, J.H. (2011). Papillation in Bacillus anthracis colonies: a tool for finding new mutators. Mol Microbiol *79*, 1276-293.

VITA

Personal Background	Christopher Ryan Evans Sherman, Texas Christian University
Education	Diploma, Sherman High School, Sherman, Texas, 2007 Bachelor of Science, Biology, Texas Christian University, Fort Worth, Texas, 2011 Master of Science, Biology, Texas Christian University, Fort Worth, Texas, 2013
Experience	Laboratory Volunteer, University of North Texas Health Science Center, Fort Worth, Texas, 2010-2011 Teaching Assistantship, Texas Christian University, Fort Worth, Texas, 2011-2012
Professional Memberships	Texas Society of Microscopy American Society of Microbiology

ABSTRACT

INVESTIGATION OF THE CLPXP PROTEASE'S CONNECTION TO *BACILLUS ANTHRACIS* CELL WALL CHARACTERISTICS

by Christopher Ryan Evans, M.S., 2013
Department of Biology
Texas Christian University

Thesis Advisor: Shauna McGillivray, Assistant Professor of Biology

We recently demonstrated that ClpX is critical for the pathogenesis and resistance to cell wall-acting antimicrobials of *Bacillus anthracis*, the causative agent of anthrax. ClpXP is an intracellular protease conserved across many bacterial species and is often associated with cellular stresses and has been implicated in the virulence of several pathogens. Antimicrobial resistance to cell wall-acting agents can result from a decrease in autolytic activity and an increase in cell wall charge or thickness. We have examined the genetic expression of autolytic and cell charge-acting genes using real-time quantitative PCR and directly measured these characteristics in a *B. anthracis* mutant lacking ClpX. We examined structural cell wall differences in our ClpX mutant using scanning and transmission electron microscopy. Our results indicate that the loss of ClpX does not affect the autolytic rate or cell wall charge of *B. anthracis*, but does result in the thinning of the cell wall.